45. Spatial Dependence of Short-period Geomagnetic Fluctuations on Oshima Island (2).

By Yoichi SASAI,

Earthquake Research Institute.

Summary

Geomagnetic variation anomaly on Oshima Island is analyzed on the basis of observations during a period from 1966 to 1967. Short-period variations in the Z component are found to be affected seriously by variations in the D component on the eastern part of the island. Parkinson vectors are determined for six stations from a number of short-period geomagnetic events having a duration time of 30 minutes or so. Electric currents induced in the sea surrounding the island are calculated on the assumption that the conductivity distribution is proportional to the actual sea-depth. The magnetic field produced by such a current distribution is also obtained and compared with the observations. The presumption in the first report, i.e. that the spatial discrepancy of short-period variations observed on Oshima Island is caused by induced currents in the sea and also that the larger scale "Central Japan Anomaly" is superposed on such a locally-induced field, seems to be supported by the present analysis.

1. Introduction

The vertical component of short-period geomagnetic fluctuations substantially differs from point to point on Oshima Island. In the previous paper[1] is investigated, in fair detail, the anomalous behaviour of Z variations along the North-South profile on the island, where many data sufficient for an analysis have been obtained. One of the most remarkable features of the anomaly is the reversal in phase between short-period Z variations as observed at the northern and southern stations. On the contrary, any noticeable differences are not found in the Sq variation. Spectral analyses of short-period disturbances in the period range from 10 minutes to 2 hours also confirm a monotonic decrease of

---

1) Y. SASAI, *Bull. Earthq. Res. Inst.*, **45** (1967), 137.

the anomalous Z component with increasing period.

It is also noticed that the maximum upward amplitude of the Z component is associated with a horizontal component of a certain direction which is peculiar to each station. Such a "preferred direction" is roughly North-East at the northernmost station KO and South at the southernmost station HA, both of which point to the nearest deep sea. All these suggest that the observed anomaly on Oshima Island is ascribable to electric currents induced in the surrounding sea by a varying external field, although no direct estimate of such a current pattern is made in the first report.

Similar phenomena which are called the "island effect" have been discovered on several islands in the vast ocean such as Christmas[2], Oahu[3], Puerto Rico[4] island and so on, and studied notably by Mason[2]. Unlike the case of these islands, the Oshima anomaly seems to be hardly explained by the island effect only and we should take account of the influence of the Central Japan Anomaly which has been investigated by Rikitake and his co-workers.[5]

It is intended in the present paper to report on the results of the observations added to those already reported in the previous paper. Observations were conducted along the E-W profile and at Futagoyama, a station at the central area of the island, from September 1966 to January 1967. Typical magnetograms at these stations will be shown in Section 2. The statistical relation between the vertical and horizontal components of short period will be investigated for each station as summarized in Section 3.

An attempt will be made in Section 4 to interpret the Oshima anomaly in terms of the induced currents in the surrounding sea. The modification of roughly uniform electric currents due to the highly resistive island is evaluated by giving the actual distribution of the sea depth around the island. The magnetic field produced by such a modified flow will be calculated and compared with the observational results.

2. Observations along the East-West Profile and at Station Futagoyama.

Three sets of portable Flux-Gate magnetometers were set at stations

2) R. G. Mason, *Geophysics Department, Imperial College of Sci. and Tech.*, **REF 63-3** (1963).
3) R. G. Mason, *Trans. Amer. Geophys. Un.*, **44** (1963), 40.
4) D. Elvers and D. Perkins, *Trans. Amer. Geophys. Un.*, **45** (1964), 46.
5) T. Rikitake, *Geophys. Jour.*, **2** (1959), 276.

Table 1. Locations of observational points, together
with their declinations.

Station	Abbr.	Long.	Lat.	Dec.
Nomashi	NO	139°11.5′E	34°43.8′N	4°50′W
Onsen Hotel	ON	24.2	45.3	9 30
Oshima Zoo	ZO	26.4	45.0	8 50
Weather Station	WE	22.5	45.7	5 10
Kowakien Hotel	KO	23.5	46.9	6 40
Habu	HA	25.9	41.0	7 50
Futagoyama	FU	24.9	42.5	——

ON, ZO and FU in September 1966. The distribution of these stations
is shown in Fig. 1, and their locations are summarized in Table 1.
Ordinary magnetograms were also available at station NO, a permanent
magnetic observatory of the Earthquake Research Institute. Unfor-
tunately, magnetometers at ZO and FU suffered some instrumental
troubles and records are available only during a period from September
to November at ZO and from November to January at FU respectively.

Fig. 2 shows typical magnetograms of the repeated occurrences of
bay-like events on October 16 along the E-W profile. A drift observed
in the Z and H component at NO would be due to temperature effects.
Corresponding to the three peaks in the H component variation, fairly
parallel changes are seen in the vertical component at NO, as reported
in the previous paper. On the other hand, the Z variation at ZO is
strongly affected by the D component variation. An upward magnetic
field is always observed there when the external field changes to the
east. A similar tendency is also, but to a less extent, seen at ON,
while the Z variation at NO seems to have no close correlation with
the D component.

At the earliest stage of the present work, in April 1966, we operated
our magnetometers along the East-West profile; at stations ZO, ON, WE
and NO. During that period we had few magnetically disturbed days,
and because of inexperience many simultaneous records were missed.
In fact, only a record of bay which occurred on April 11 is available
and shown in Fig. 3. No discrepancy in the Z component between these
stations can be seen in the figure. The small amplitude of the D
component should be noticed in this case. Along the E-W profile, the
anomalous Z variation appears on the eastern side of the island, ac-
companied with the D component. When the external field changes in
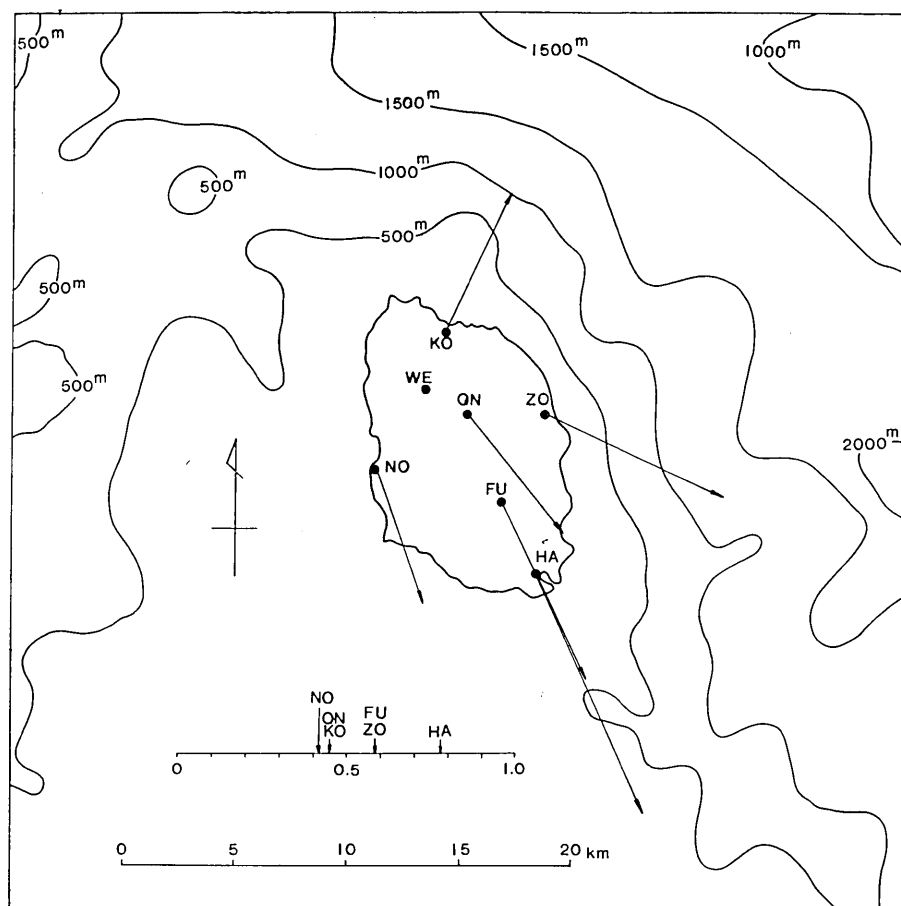
Y. Sasai

Fig. 1. Localities of the observational points. Bathymetric contours are also
shown. Arrows indicate "induction arrows".

the N-S direction, the Z variation is nearly the same for all these
stations and characterized by its large amplitude as well as marked
parallelism with the H component.

In Fig. 4 is shown an outstanding magnetic event observed at FU,
the magnetogram being compared with those at NO and ON. Since the
horizontal component variations are nearly the same at all stations, only
the horizontal magnetograms at NO are shown in the figure. The Z
component variation is fairly in phase with the H at FU and NO, but
its amplitude is substantially larger at FU.

The Sq variation on November 8, 1966 at stations ZO, ON, NO and
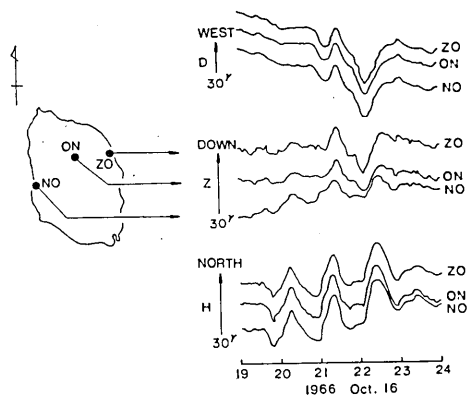
Fig. 2. Repeated occurrences of bay-like events on October 16 along the E-W profile. Arrows indicate 30 gammas.
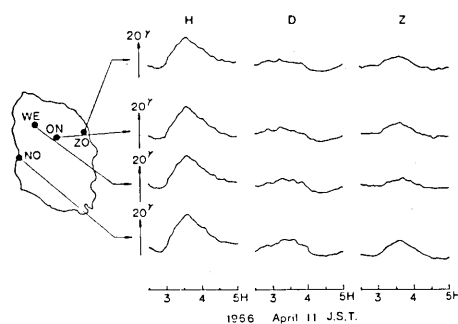

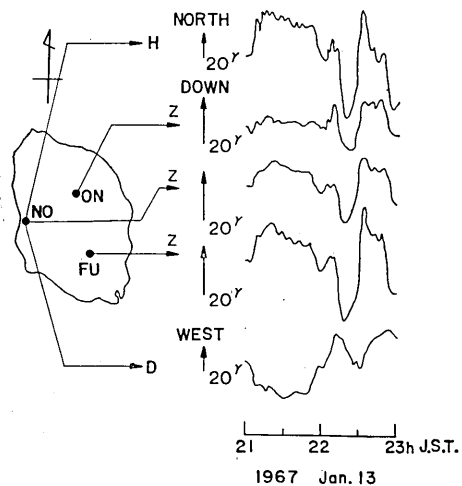Fig. 3. A bay observed on April 11. Arrows indicate 20 gammas.

Fig. 4. An outstanding magnetic event observed at ON, NO and FU on January 13, 1967. Arrows indicate 20 gammas.
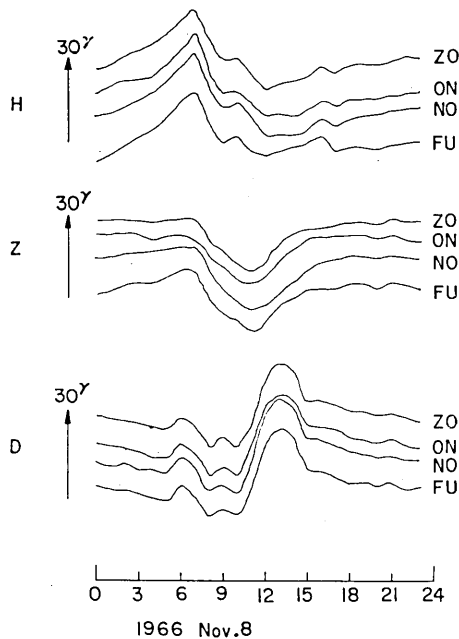

Fig. 5. The Sq variation on November 8, 1966.

FU are compared. Hourly values of the three components are read off and plotted in Fig. 5. Similar to the case of the N-S profile, the Sq variation is almost the same at all stations[1].

3. Characteristics of the Anomalous Z Component of Short-period Fluctuations at Each Station.

The anomalous Z variation on Oshima Island has a clear-cut anisotropy with respect to the horizontal direction of the varying external field. A preliminary investigation of the indicated anisotropy was made for the station KO and HA in the first report. Short-period disturbance vectors were found to be confined on a plane (so-called a preferred plane) at these two stations. A similar tendency was also confirmed for other stations ZO, NO, NO and FU. As for station WE, we have no sufficient data of short-period variations for determining the preferred plane. Adding some new data to the previous ones, the results for KO and HA were reexamined, and were slightly different from that described in the first paper.

Short-period geomagnetic events having a duration time 10 to 40 minutes were selected and read off their maximum amplitudes ΔZ, ΔH and ΔD. Events for which the maximum epoch of both the H and D variation occurs at the same time were chosen. The phase lag of the Z variation is negligibly small for the period range under consideration.

The amplitude ratio $\Delta Z/\Delta D$ was plotted against $\Delta H/\Delta D$ for each station in Fig. 6(a) for station KO, (b) ON, (c) ZO, (d) NO, (e) FU and (f) HA respectively. As shown in the figures, $\Delta Z/\Delta D$ is linearly correlated with $\Delta H/\Delta D$; hence, the following expression is permissible for the relation between the vertical and the two horizontal components:

$$\Delta Z = A \cdot \Delta H + B \cdot \Delta D \tag{1}$$

Coefficients A and B may be obtained by the least square method.

Rikitake and Yokoyama[6] first noticed the existence of the preferred plane at some Japanese magnetic observatories in the course of their study on the Central Japan Anomaly. Parkinson[7],[8] investigated short-period fluctuations observed in Australia and found a similar tendency at near-coast observatories. He devised a well-known graphical representation (so-called Parkinson vector) of the preferred plane characterized by coefficients A and B in eq. (1). A Parkinson vector is defined as the horizontal projection of the downward unit vector normal to the plane.

A slightly different representation is adopted here for convenience's

6) T. Rikitake, and I. Yokoyama, *Bull. Earthq. Res. Inst.*, **33** (1955), 297.

7) W. D. Parkinson, *Geophys. Jour.*, **2** (1959), 1.

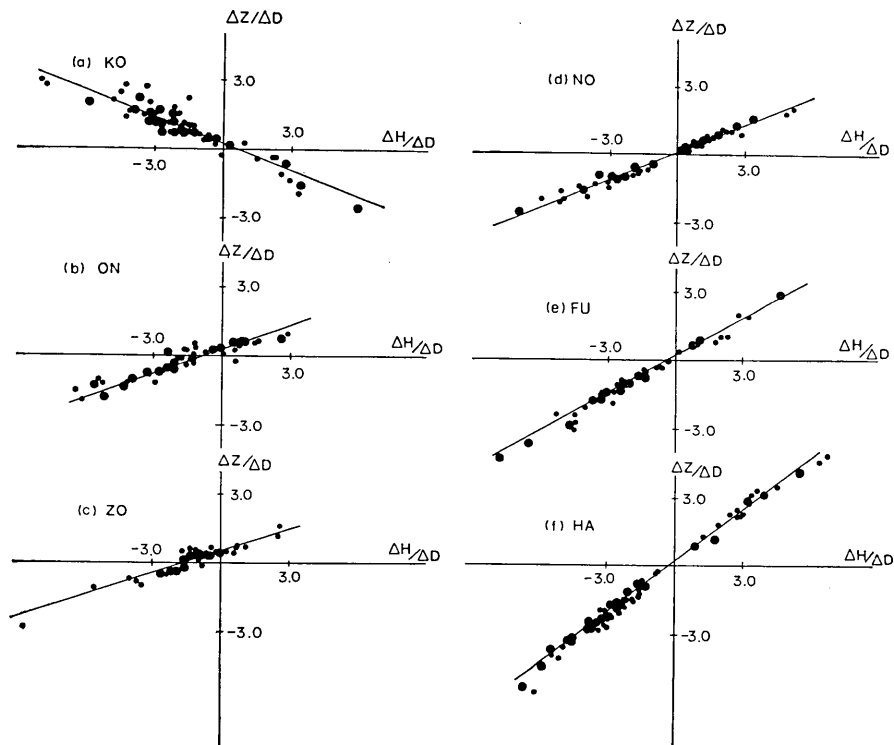8) W. D. Parkinson, *Geophys. Jour.*, **6** (1962), 441.

Fig. 6. $\Delta Z/\Delta D$ values plotted against $\Delta H/\Delta D$ at (a) KO, (b) ON, (c) ZO, (d) NO, (e) FU and (f) HA.

sake.   The modified Parkinson vector or the "induction arrow" $\vec{S}$ is given as follows;

$$S = \sqrt{A^2 + B}$$

$$\phi_m = \tan^{-1} \frac{B}{A} \qquad (2)$$

where S is the magnitude of the Vector $\vec{S}$, and ϕ_m, its azimuth measured counterclockwise from magnetic south.   From eq. (1), the vector $\vec{S}$ shows the direction of maximum upward Z variation toward which the horizontal component increases.   When the horizontal component ΔR increases to any particular direction, the amplitude ratio $\Delta Z/\Delta R$ is given by the projected length of the vector $\vec{S}$ onto that direction.

In Table 2 are listed coefficients A, B, together with their standard

Table 2.　Induction Arrows on Oshima Island.

Station	A	B	S	ϕ_m	ϕ
KO	-0.39 ± 0.03	0.24 ± 0.03	0.46	S 147.8° E	N 25.5° E
ON	0.35 ± 0.02	0.28 ± 0.03	0.45	38.7	S 48.2 E
ZO	0.33 ± 0.02	0.49 ± 0.03	0.59	56.2	65.0
NO	0.41 ± 0.01	0.10 ± 0.01	0.42	13.4	18.2
FU	0.56 ± 0.01	0.18 ± 0.02	0.58	17.9	25.7
HA	0.75 ± 0.01	0.23 ± 0.03	0.78	16.9	24.7

deviations, S, ϕ_m and ϕ for each station. ϕ is the orientation of the vector $\vec{S}$ when the declination at each station is taken into account. $\vec{S}$'s for respective stations are illustrated in Fig. 1. Bathymetric contours are also shown there.

Induction arrows at KO, ZO and ON tend to point the nearest deep sea. The "island effect" due to the oceanic induced currents would be the best explanation for such a tendency. The direction of the vector $\vec{S}$ at NO is, however, far beyond comprehension so far as we persist in accounting for the Oshima anomaly solely in terms of the simple "island effect". From such a viewpoint, the arrow at NO is expected to turn to the west. The large values of S's at FU and HA (which means the large amplitude of Z component) are also unreasonable when the presence of the shallow sea south of the island is taken into account.

4. Electric Currents Induced in the Sea around Oshima Island.

In view of the fact that the preferred planes at KO, ZO and HA dip toward the center of the island, the sea water around Oshima Island seems to react as a nearly perfect conductor against a varying external field having a period of a few tens of minutes, so that magnetic lines of force tend to be parallel to the sea surface. In order to reach a clear-cut understanding of the island effect, it is desirable to estimate electric currents induced in the surrounding sea.

In case of electromagnetic induction within a vast sea, the sea can be regarded as an infinitely thin conducting sheet. A comprehensive theory of electromagnetic induction in non-uniform thin sheets and shells was given by Price[9]. Rikitake[10] devised a method for estimating locally

9)　A. T. PRICE, *Quart. Jour. Mech. Appl. Math.*, **2** (1949), 283.
10)　T. RIKITAKE, *Unpublished manuscript*, (1967).

induced currents in a sheet having a less conducting area at its center. The method can be applied to an island in the sea. Since no reference is available as yet, an outline of the method is given in the following.

According to the theory of electromagnetic induction within a non-uniform plane sheet, the current function Ψ is governed by,

$$\rho \nabla^2 \Psi + \operatorname{grad} \rho \operatorname{grad} \Psi = \frac{\partial}{\partial t} (Z_e + Z_i)_{z=0} \tag{3}$$

where

$$\nabla^2 = \frac{\partial^2}{\partial x^2} + \frac{\partial^2}{\partial x^2} \tag{4}$$

and the sheet is assumed at $z=0$.

If it is assumed that the island is non-existent, the equation becomes

$$\rho_0 \nabla^2 \Psi_0 + \operatorname{grad} \rho_0 \operatorname{grad} \Psi_0 = \frac{\partial}{\partial t} (Z_e + Z_{io})_{z=0} \tag{5}$$

in which the subscript 0 denotes quantities when there is no island. ρ_0 is not necessarily uniform, so that we may investigate electromagnetic induction in a large-scale structure from which local irregularity due to an island is removed.

On making difference between (3) and (5), we can derive an equation that controls the anomalous current function which is given rise to by the island.

Putting

$$\begin{aligned} \psi &= \Psi - \Psi_0 \\ z_i &= Z_i - Z_{io} \end{aligned} \tag{6}$$

we obtain

$$\rho \nabla^2 \psi + \operatorname{grad} \rho_0 \cdot \operatorname{grad} \psi = -(\rho - \rho_0) \nabla^2 \Psi_0 - \operatorname{grad} (\rho - \rho_0) \cdot \operatorname{grad} \Psi_0 + \left(\frac{\partial z_i}{\partial t}\right)_{z=0} \tag{7}$$

The anomalous area is generally a very small one. In such a case, the effect of self-induction would be small so that $\dfrac{\partial z_i}{\partial t}$ on the righthand-side of (7) can be ignored to a high degree of approximation. Since Ψ_0 for a specified inducing field is solved from (5), the righthand-side of (7) then becomes specified. We may thus determine the anomalous current

function by solving (7) from which $\dfrac{\partial z_i}{\partial t}$ is dropped.

$$\rho \nabla^2 \psi + \operatorname{grad} \rho \cdot \operatorname{grad} \psi = -(\rho - \rho_0) \nabla^2 \Psi_0 - \operatorname{grad}(\rho - \rho_0) \cdot \operatorname{grad} \Psi_0 \qquad (8)$$

ψ should vanish at infinity. Although there seems no way to analytically tackle the equation, (8) may be solved by some numerical method such as the relaxation method.

In the present case, Oshima Island and the surrounding sea is covered with a square mesh of 1 km spacing. The sea depth is read at each grid point for a 40×40 km square from a chart published by the Hydrographic Office, Marine Safety Board, Japan. The integrated resistivity ρ of the sea is given by,

$$\rho = \int_0^D \frac{1}{\sigma_0} ds = \frac{D}{\sigma_0} \qquad (9)$$

where σ_0 is the electrical conductivity of sea water ($\sigma_0 = 4 \times 10^{-11}$ emu) and D the sea depth at the point. The island should have a finite integrated resistivity, which is taken here tentatively as a hundred times larger value than the 1 km-depth sea. Hence, the influence of the island is equivalent to that of a shoal of 10 meter's depth.

It is difficult, however, to estimate the "regional" current function Ψ_0 governed by eq. (5). Since the average sea depth at the boundaries of the square is roughly 1 km as shown in Fig. 1, the writer adopted here an ocean of 1 km depth as a broad conductivity structure around the area concerned. Ψ_0 can easily be obtained in this case. (See Rikitake[11])

Taking the x- and y- axes northward and westward respectively, and supposing that an inducing field arises from sources lying in a space $z > 0$, a typical form of inducing potential, which is uniform in the y-direction, can be written as:

$$W_e = A_0 e^{\lambda z} \sin \lambda x \qquad (10)$$

The potential of the magnetic field produced by electric currents induced in the uniform plane sheet is

$$W_{io} = \begin{cases} B_0 e^{-\lambda z} \sin \lambda x & \text{for } z > 0 \\ -B_0 e^{-\lambda z} \sin \lambda x & \text{for } z < 0 \end{cases} \qquad (11)$$

11) T. Rikitake, *Electromagnetism and the Earth's Interior*, Elsevier Pub. Co. Amsterdam (1966).

and B_0 is given as:

$$B_0 = 2\pi p (\rho_0 \lambda + 2\pi p)^{-1} A_0 \qquad (12)$$

where $p = \dfrac{\partial}{\partial t}$

Similar expressions are obtained for the westward inducing field, replacing x with y in eq. (10) and (11).

For convenience, A_0 is taken here as unity. For a periodic field having a form of $e^{i\omega t}$, p is replaced by $i\omega (i = \sqrt{-1}, \omega = 2\pi/T, T$: period) Then B_0 is rewritten as follows:

$$B_0 = U + iV \qquad (13)$$

where

$$U = \frac{1}{1+\alpha^2}, \qquad V = \frac{\alpha}{1+\alpha^2}, \qquad \alpha = \frac{\rho_0 \lambda}{2\pi\omega} \qquad (14)$$

The current function Ψ_0 is defined by

$$\Psi_0 = \frac{1}{2\pi} (W_{io})_{z \to +0} = \frac{1}{2\pi} (U + iV) \sin \lambda x \qquad (15)$$

The time variation of the anomalous current function ψ is exactly the same as that of Ψ_0 because the self-induction term $\dfrac{\partial z_i}{\partial t}$ is excluded in eq. (8). How the in-phase (U) and out-of-phase part of (V) of B_0 change with the period is studied in the following.

ρ_0 is estimated as 2.5×10^5 e.m.u. from eq. (9). The wave number of the external field λ is taken as $10^{-8}\,\mathrm{cm}^{-1}$, which is an appropriate value for short-period disturbances in the middle latitude. Induction curves of the present model are illustrated in Fig. 7, where U and V are given as functions of period T. As shown in the figure, the out-of-phase part V is very small compared with U for the period shorter than 1 hour. Induction ar-
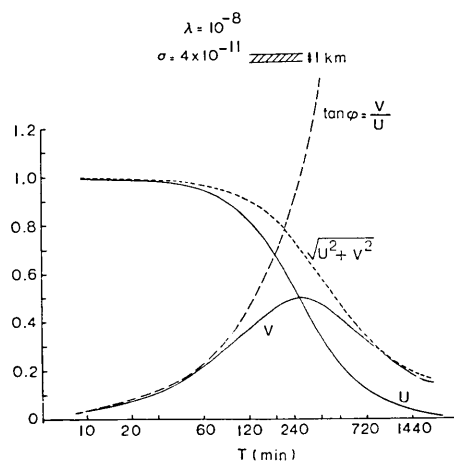

Fig. 7. Induction curves for a uniform thin sheet-conductor.

rows are determined for magnetic events having a duration time 10 to 40 minutes. Then 30 minutes can be regarded as a representative period of the short-period disturbances dealt with in Section 3. U and V are calculated as 0.987 and 0.113 respectively for $T=30$ min. Hence, the phase delay of the induced field behind the inducing field amounts to only 0.5 min. This is consistent with that the observed phase lag of the Z component is negligibly small.

The difference form of the eq. (8) is solved numerically by the relaxation method on an electronic computer. The residual $R(j, k)$ at a point (j, k) is given as:

$$
\begin{aligned}
R(j, k) = & R1(j, k) \cdot \psi(j-1, k) + R2(j, k) \cdot \psi(j, k+1) \\
& + R3(j, k) \cdot \psi(j+1, k) + R4(j, k) \cdot \psi(j, k-1) \\
& - R5(j, k) \cdot \psi(j, k) + 2d^2 f(j, k)
\end{aligned} \tag{16}
$$

where

$$
\begin{aligned}
R1(j, k) &= \rho_{j-1,k} + \rho_{j,k} \\
R2(j, k) &= \rho_{j,k+1} + \rho_{j,k} \\
R3(j, k) &= \rho_{j-1,k} + \rho_{j,k} \\
R4(j, k) &= \rho_{j,k-1} + \rho_{j,k} \\
R5(j, k) &= \rho_{j-1,k} + \rho_{j,k+1} + \rho_{j+1,k} + \rho_{j,k-1} + 4\rho_{j,k} \\
f(x, y) &= (\rho - \rho_0)\nabla^2 \Psi_0 + \text{grad}\,(\rho - \rho_0) \cdot \text{grad}\,\Psi_0
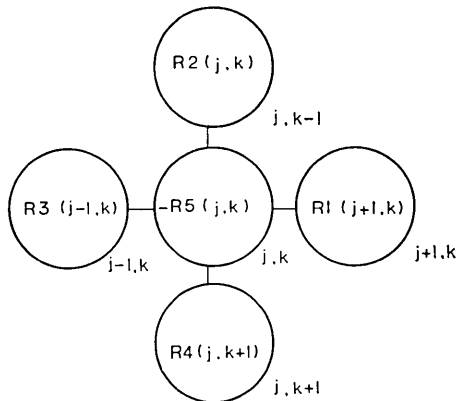\end{aligned} \tag{17}
$$

Fig. 8. The relaxation pattern which shows changes of residuals at a point (j, k) and its four clesest neighbours when $\psi(j, k)$ increases by +1.

and d is the grid interval. In Fig. 8 is given the relaxation pattern which shows the changes of residuals at a point (j, k) and its four closest neighbors when $\psi(j, k)$ increases by +1. At the boundaries of the square, ψ is taken to be zero.

The magnetic potential on the upper side of the sheet conductor becomes

$$
W_0(x, y, 0) = 2\pi \Psi(x, y) \tag{18}
$$

and the horizontal components of the magnetic field at $z=0$ are given as:

$$X(x, y, 0) = -\frac{\partial W_0}{\partial x}$$

$$Y(x, y, 0) = -\frac{\partial W_0}{\partial y} \tag{19}$$

while the vertical component is given by the potential theory as:

$$Z(x, y, 0) = -\frac{1}{2\pi} \int_0^{2\pi} \int_0^\infty (W_0 - U_0) \frac{dr d\theta}{r^2} \tag{20}$$

in which U_0 denotes the value of W_0 at a certain point on the sheet which is the origin of a polar coordinate r and θ.
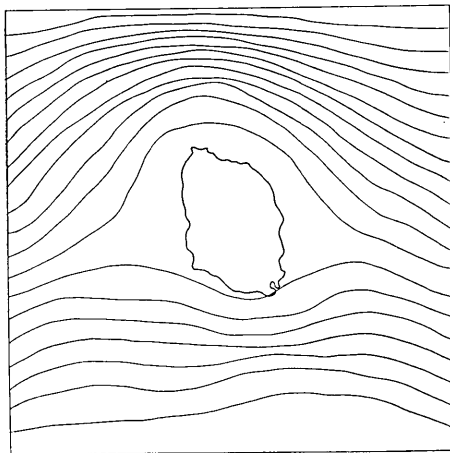
In Figs. 9 and 10 are shown the induced current pattern for the

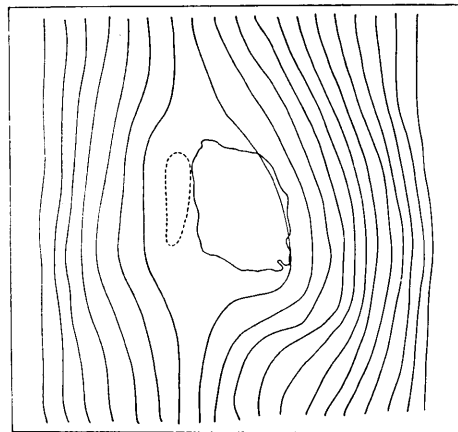Fig. 9. Induced current pattern for the northward inducing field.

Fig. 10. Induced current pattern for the westward inducing field.

northward and westward inducing field respectively. It is clearly seen that electric currents are deflected by the poorly-conducting island. It should also be noticed that intense currents tend to flow in the northern and eastern deep sea.

The X(north-), Y(west-) and Z(downward) components of the induced field are calculated with the aid of relations from (18) to (20). The inducing field can be easily obtained by differentiating its potential given by eq. (10). Fig. 11 (a), (b) and (c) show the in-phase part of the Z, X and Y component of the total magnetic field when the external field changes in the N-S direction. The field intensity is normalized in such a way that $A_0\lambda$ is equal to unity. The out-of-phase part is negligibly
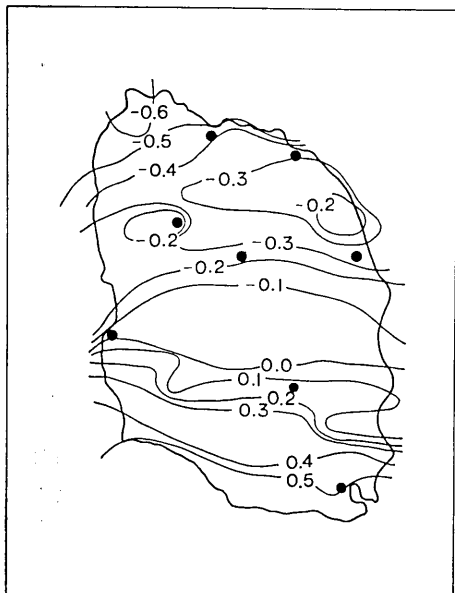
Fig. 11 (a). In-phase part of the Z component of the total magnetic field for the northward inducing field.
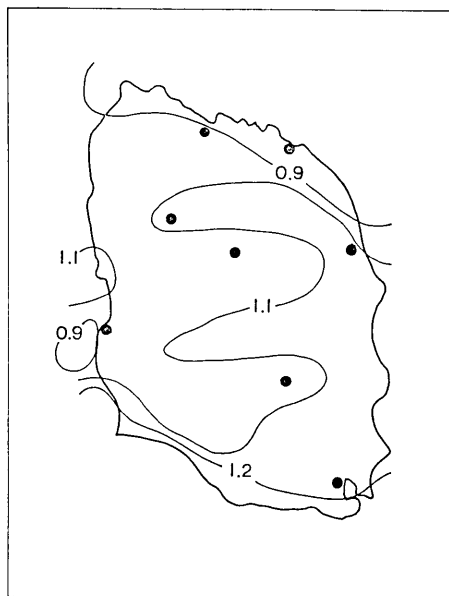

Fig. 11 (b). In-phase part of the X component of the total magnetic field for the northward inducing field.
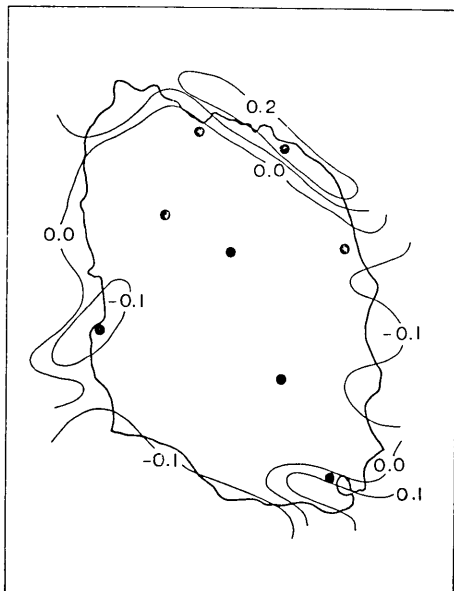

Fig. 11 (c). In-phase part of the additional Y component of the total magnetic field for the northward inducing field.

small compared with the in-phase one. As shown in Fig. 11 (a), the induced Z component changes its sign between the northern and southern part of the island. When the horizontal component changes in the north direction, the X component is upward on the northern side and downward on the southern side of the island. Such a tendency coincides with the observed feature of the anomaly. It would be noteworthy that the calculated anomalous Z component becomes zero at station NO. As for the horizontal variations, the X component is roughly the same all over the island and the additional Y component is very small.
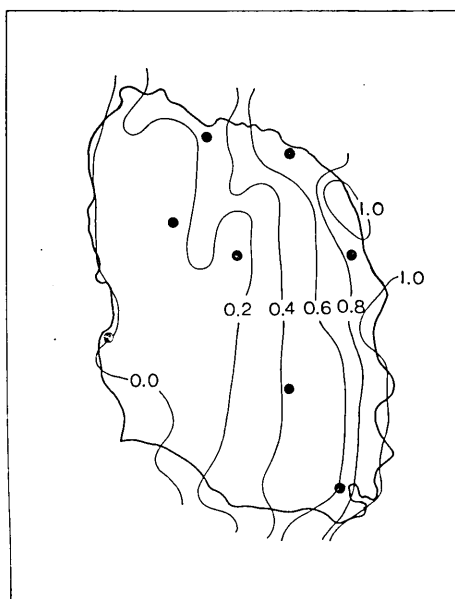
Fig. 12 (a). In-phase part of the *Z* component of the total magnetic field for the westward inducing field.
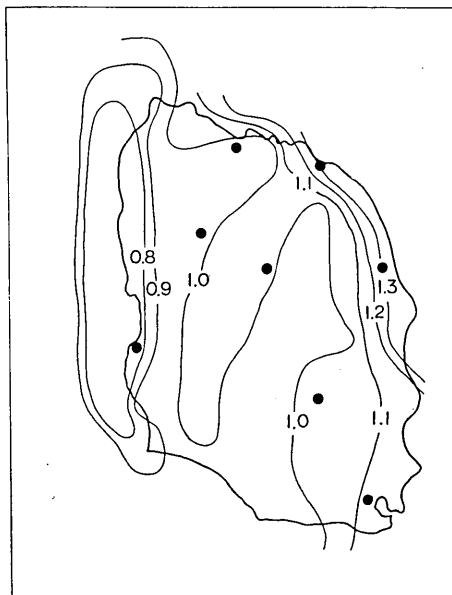

Fig. 12 (b). In-phase part of the *Y* component of the total magnetic field for the westward inducing field.
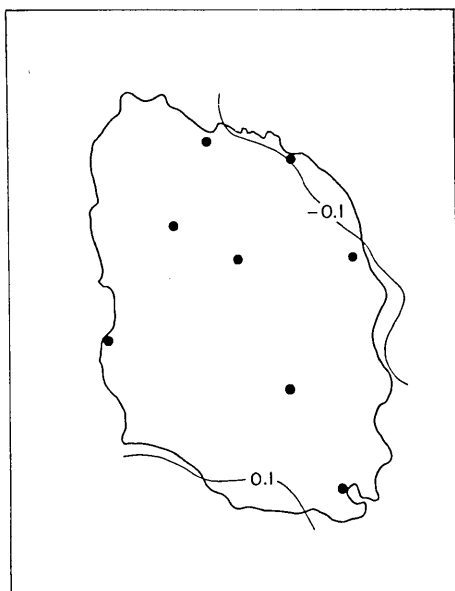

Fig. 12 (c). In-phase part of the additional *X* component of the total magnetic field for the westward inducing field.

In Fig. 12 (a), (b) and (c) are given the in-phase part of the Z, Y and X component of the total field for the westward inducing field. When the horizontal component increases in the west direction, the Z component shows more or less downward increase on the island with much augmentation along the east coast. The zero variation contour of Z runs along the west coast-line of the island and again, the Nomashi Observatory (NO) is not affected by the oceanic induced currents.

In-phase and out-of-phase parts (denoted by the subscript u and v respectively) of total field component are summarized for each

Table 3 (a). In-phase (u) and out-of-phase (v) parts of
the total field components for the northward
inducing field.

Station	$\varDelta Zu$	$\varDelta Zv$	$\varDelta Xu$	$\varDelta Xv$	$\varDelta Yu$	$\varDelta Xv$
KO	−0.42	−0.04	0.92	−0.01	0.00	0.00
ON	−0.21	−0.02	1.00	0.00	0.00	0.00
ZO	−0.32	−0.04	1.10	0.01	0.00	0.00
NO	0.00	0.00	0.92	−0.01	−0.08	−0.01
FU	0.16	0.02	1.00	0.00	0.00	0.00
HA	0.48	0.05	1.10	0.01	0.10	0.01
SE	−0.30	−0.03	0.78	−0.02	0.20	0.02
WE	−0.15	−0.01	1.10	0.01	0.10	0.01

Table 3 (b). In-phase (u) and out-of-phase (v) parts of
the total field components for the westward
inducing field.

Station	$\varDelta Zu$	$\varDelta Zv$	$\varDelta Xu$	$\varDelta Xv$	$\varDelta Yu$	$\varDelta Yv$
KO	0.25	0.03	0.00	0.00	1.00	0.00
ON	0.15	0.02	0.00	0.00	1.10	0.01
ZO	0.90	0.10	0.00	0.00	1.30	0.04
NO	0.00	0.00	0.00	0.00	0.80	−0.02
FU	0.45	0.06	0.00	0.00	1.10	0.01
HA	0.60	0.08	0.00	0.00	1.13	0.01
SE	0.72	0.08	−0.10	−0.01	1.31	0.03
WE	0.11	0.01	0.00	0.00	1.00	0.00

station in Table 3 (a) for the northward and 3 (b) for westward inducing
field respectively. Since the out-of-phase parts are negligibly small, the
calculated secondary part As and Bs would be represented as follows:

$$As = \left(\frac{\varDelta Zu}{\varDelta Xu}\right)_{\mathrm{NORTH}}, \qquad Bs = \left(\frac{\varDelta Zu}{\varDelta Yu}\right)_{\mathrm{WEST}} \tag{21}$$

$\bar{A}$ and $\bar{B}$, the projection of the vector $\vec{S}$ onto the geographic N-S
and E-W direction, represent the observed field ratio $\varDelta Z/\varDelta X$ and $\varDelta Z/\varDelta Y$
respectively. $\bar{A}$ and $\bar{B}$ are given by

$$\begin{aligned} \bar{A} &= S\cos\phi = A\cos D - B\sin D \\ \bar{B} &= S\sin\phi = A\sin D + B\cos D \end{aligned} \tag{22}$$

Table 4. Observed field ratios ($\bar{A}, \bar{B}$), calculated secondary parts (A_s, B_s) and expected field ratios (A', B': See next section) at each station.

Station	$\Delta Z/\Delta X$			$\Delta Z/\Delta Y$		
	$\bar{A}$	A_s	A'	$\bar{B}$	B_s	B'
K O	−0.42	−0.46	−0.06	0.19	0.25	0.35
O N	0.30	−0.21	0.16	0.33	0.14	0.23
Z O	0.25	−0.29	0.05	0.53	0.69	0.77
N O	0.40	0.00	0.40	0.13	0.00	0.13
F U	0.53	0.16	0.53	0.25	0.41	0.50
H A	0.71	0.44	0.78	0.33	0.53	0.62
S E	—	−0.38	0.09	—	0.55	0.63
W E	—	−0.14	0.20	—	0.11	0.21

$\bar{A}, \bar{B}, As$ and Bs are summarized in Table 4. The discrepancy between the observed and calculated field ratios is large in the case of northward inducing field. This means that the Oshima anomaly cannot be explained by electric currents induced in the surrounding sea only.

5. Discussion

The present model calculations are based on an idea that the island effect on short-period geomagnetic variations is caused by a deflected current flow around the island of an otherwise uniform current induced in a vast ocean. The actual situation around Oshima Island is very much different from such an idealized one, because it is very close to Honshu Island, the main land of Japan. Rikitake[12] investigated electromagnetic induction within a non-uniform spherical shell simulating the large-scale land sea distribution over the earth. He showed that the induced currents tend to be deflected from the low-conducting continental areas and to encircle the oceanic areas. Hence, the "regional current function" Ψ_0 around Oshima Island is expected to be not so uniform as that of 1 km-depth sea. There are some additional uncertainties in assumptions adopted in the model calculations, i.e. the wavelength of the external field, the conductivity contrast between land and sea, and the like are taken rather arbitrarily.

It seems to the writer, however, that the "island effect" would

---

12) T. Rikitake, *Bull. Earthq. Res. Inst.*, **45** (1967), 1229.

essentially be controlled by the very local conductivity structure just around the island. The general tendency obtained in the previous section seems qualitatively acceptable, especially in the case of the westward inducing field. Although the anomalous Z component is expected to be zero at NO from our model experiment, a large value of A is obtained there.

In the first report, the writer presumed that the Oshima anomaly is composed of two parts: the primary and secondary one. The latter is the locally induced field which causes the observed spatial discrepancies of the short-period Z component, while the former is regarded as the regional inducing and induced fields, uniform over the island. The writer presumes that Oshima Island belongs to the anomalous area of the Central Japan Anomaly[5] characterized by a large Z component of short-period variations when the horizontal component changes in the N-S direction. If so, the primary part has a large downward Z component with the northward horizontal variation, and hence it would intensify the secondary part at the southern part of the island and oppose it at the north. The behaviour of the Z component variation at NO is expected most likely to represent the primary part on Oshima Island, because the influence of the surface-induced currents is least there in the present model.

If we assume that the primary part can be regarded as the field ratios $\bar{A}$ and $\bar{B}$ at NO and the secondary part at each station as As and Bs given by eq. (21), the expected field ratios A' and B' are given as follows:

$$\begin{aligned} A' &= Ap + As \\ B' &= Bp + Bs \end{aligned} \tag{23}$$

where Ap and Bp are the expected primary part when the differences in the amplitude of horizontal component are taken into account and given by

$$\begin{aligned} Ap &= \left(\frac{\Delta X_{u,\mathrm{NO}}}{\Delta X_u} \right)_{\mathrm{NORTH}} \bar{A}_{\mathrm{NO}} \\ Bp &= \left(\frac{\Delta Y_{u,\mathrm{NO}}}{\Delta Y_u} \right)_{\mathrm{WEST}} \bar{B}_{\mathrm{NO}} \end{aligned} \tag{24}$$

For the northward inducing field, the observed field ratio $\bar{A}$, the calculated secondary part As and the expected field ratio A' are plotted

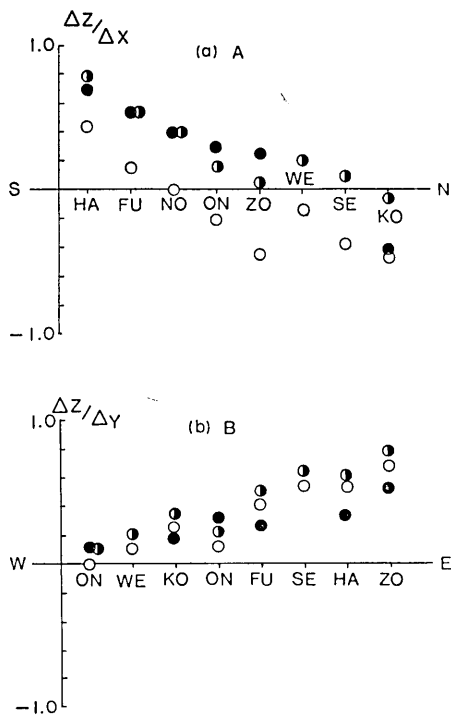in Fig. 13 (a). In Fig. 13 (b) are given $\bar{B}, Bs$ and B'. General agreement between the expected field ratio and the observed one is rather poor. The former is more irregular and larger in amplitude than the observed ratios. Hence, the secondary part calculated with the parameters assumed seems to be an overestimate.

In the present discussion, the interaction between the primary and secondary part is ignored. In spite of intensive studies over many years we have not arrived at a physically acceptable understanding of the cause of the Central Japan Anomaly yet. It seems very likely, however, that this anomaly would be due to some inhomogeneous conductivity structure under the Japan Islands, although the contribution of oceanic induced currents should also be important in some cases. The mutual electromagnetic coupling between such an underground structure and the conducting surface should be taken into account.

Although it is beyond the scope of this paper to conduct such a detailed study, it is surmised that the said coupling might not be very large because the size of the island is smaller than the depth of the top-surface of the underground conductor.

Fig. 13. The observed field ratio (black circle), the calculated secondary part (hollow circle) and expected field ratio (semi-black circle): (a) for the northward inducing field, (b) for the westward inducing field.

In conclusion, the spatial discrepancy of the short-period Z variations on Oshima Island can be explained mainly by the induced current in the surrounding sea. More accurate discussion will be possible by refining the present model in the way argued in this section.

6. Acknowledgements

---

45. 伊豆大島における地磁気短周期変化の異常（2）

地震研究所　笹　井　洋　一

　伊豆大島において1966年4月より翌年1月まで，携帯用フラックスゲイト型磁力計を用い，地磁気変化の同時観測を行なつた．その結果，短周期変化の鉛直成分が島内各所で著しい差を示すことが見出され，南北のプロファイルについての解析結果を前報で報告した．今回は観測期間後半の東西のプロファイルについてまとめてある．島の東側においては，西向きの磁場変化に伴なつて大きな下向きの Z 成分が観測される．しかし島の西側では，東西方向の磁場変化に伴なう Z 成分の異常は認められない．

　周期30分前後の短周期変化について，3成分の最大振幅を読みとつてみると，変化ベクトルは各観測点に固有な平面上にのる傾向が見られる．この平面の傾き，方位から，各観測点で北向き及び西向きに水平成分が変化した時，期待される Z 成分の振幅が得られる．

　前報において，伊豆大島の異常は，外部磁場の変化によつて海水中に誘導された電流が，不良導体である島を避けて流れるために起る「離島効果」であろう，と推定した．これを確かめるために，島の周辺の海の深さに比例した電気伝導度分布を持つた不均質薄層の電磁感応を計算し，前述の観測結果と比べてみた．その結果は東西方向に磁場が変化した場合はかなりよく合うが，南北方向の時に大きなくいちがいが出る．これを説明するためには，伊豆大島一帯で南北方向に磁場が変わつた場合に大きな Z 成分が生じていると考えなくてはならない．このような傾向は Central Japan Anomaly として本州中央部太平洋岸に見られる異常に他ならない．結局，第一報で述べたように，伊豆大島で観測される異常は，日本列島中央部異常と「離島効果」が重なつたものと考えられる．

　なお，この研究を進めるにあたつて伊豆大島現地の多くの方々にお世話になつた．特に観測のために種々便宜をはかつて下さつた大島温泉ホテルの小川氏，小湧園ホテルの吉田氏，気象庁大島測候所，運輸省大島航空標識所の所員の方々，また大島第三中学校の先生方に深く感謝いたします．